Synchronization of a Josephson junction array in terms of global variables

Vladimir Vlasov* and Arkady Pikovsky
Department of Physics and Astronomy, Potsdam University, 14476 Potsdam, Germany
(Received 8 April 2013; published 12 August 2013)

We consider an array of Josephson junctions with a common LCR load. Application of the Watanabe-Strogatz approach [Physica D **74**, 197 (1994)] allows us to formulate the dynamics of the array via the global variables only. For identical junctions this is a finite set of equations, analysis of which reveals the regions of bistability of the synchronous and asynchronous states. For disordered arrays with distributed parameters of the junctions, the problem is formulated as an integro-differential equation for the global variables; here stability of the asynchronous states and the properties of the transition synchrony-asynchrony are established numerically.

DOI: 10.1103/PhysRevE.88.022908 PACS number(s): 05.45.Xt, 74.81.Fa

I. INTRODUCTION

Synchronization in populations of coupled oscillators is a general phenomenon observed in many physical systems (cf. recent experimental studies of optomechanical, micromechanical, electronic, mechanical, and chemical oscillators [1]). Synchronization effects are also ubiquitous in biology and social sciences. One of the basic examples of oscillating physical systems that being coupled synchronize are Josephson junctions [2]. In theoretical studies of the Josephson junction arrays one typically either performs direct numerical simulation of the microscopic equations (see, e.g., Ref. [3]) or reduces the problem to the standard Kuramoto-type model [4–6].

Quite remarkable in this respect is Ref. [7], where a careful comparison of the microscopic modeling and the reduced Kuramoto-type model has been performed. The authors demonstrated that a hysteretic transition to synchrony in an array of Josephson junctions can be explained by a Kuramoto-type modeling (where usually the transition is not hysteretic), if in its derivation one self-consistently accounts for changes of the oscillator parameters.

Our aim in this paper is to shed light on the hysteretic transitions to synchrony in Josephson arrays by studying the equations for global variables. In this approach, which is based on the seminal papers by Watanabe and Strogatz (WS) [8,9], it is possible to formulate exact low-dimensional equations for the array, without using approximate reduction to the Kuramoto model. The paper is organized as follows. First, we formulate the equations for the array of *identical* junctions via the global variables. Analysis of these equations shows regions of bistability asynchrony-synchrony and the hysteretic transitions. Then we proceed to *nonidentical* junctions, where the equations are of more complex form. Here we analyze stability of asynchronous states and show numerically that the transition to synchrony is also hysteretic.

II. IDENTICAL JUNCTIONS

A. Formulation in terms of global variables

We start with formulating the system of equations for the Josephson junction series array with a LCR load. Our setup is the same as in Refs. [4–6]; the equations for the junction phases φ_i and the load capacitor charge Q read

$$\frac{\hbar}{2er}\frac{d\varphi_i}{dt} + I_c \sin\varphi_i = I - \frac{dQ}{dt}, \quad i = 1,\dots,N,$$
$$L\frac{d^2Q}{dt^2} + R\frac{dQ}{dt} + \frac{Q}{C} = \frac{\hbar}{2e}\sum_{i=1}^{N}\frac{d\varphi_i}{dt}. \tag{1}$$

Here N is the number of junctions, described by a resistive model with critical current I_c and resistance r, while L, C, R are parameters of the LCR load. It is convenient to introduce dimensionless variables according to

$$\omega_c = 2erI_c/\hbar, \quad t^* = \omega_c t,$$
$$Q^* = \omega_c L^* Q/I_c, \quad I^* = I/I_c, \tag{2}$$
$$R^* = R/rN, \quad L^* = \omega_c L/rN, \quad C^* = N\omega_c rC,$$

and to rewrite the system (1) in a dimensionless form (dropping the asterisks for simplicity):

$$\dot\varphi_i = I - \frac{1}{L}\dot Q - \sin\varphi_i, \tag{3a}$$
$$\ddot Q + \frac{R}{L}\dot Q + \frac{Q}{Lc} = \frac{1}{N}\sum_{i=1}^{N}\dot\varphi_i. \tag{3b}$$

Furthermore, to have equations in the canonical form with all derivatives on the left-hand side, it is suitable to substitute the expressions for $\dot\varphi_i$ from (3a) into the equation for the load (3b). Thus, the system (4) is obtained from the system (3):

$$\dot\varphi_i = I - \epsilon\dot Q - \sin\varphi_i,$$
$$\ddot Q + \gamma\dot Q + \omega_0^2 Q = I - \frac{1}{N}\sum_{i=1}^{N}\sin\varphi_i, \tag{4}$$

where $\epsilon = 1/L^*$, $\gamma = (R^*+1)/L^*$, and $\omega_0 = 1/\sqrt{L^*C^*}$.

The global coupling can be represented through the complex mean field (Kuramoto order parameter)

$$Z = re^{i\theta} = \frac{1}{N}\sum_{i=1}^{N}(\cos\varphi_i + i\sin\varphi_i),$$
$$\mathrm{Im}(Z) = \frac{1}{N}\sum_{i=1}^{N}\sin\varphi_i, \tag{5}$$

*mr.voov@gmail.com

and the equations for the junction phases can be written as

$$\dot{\varphi}_i = I - \epsilon \dot{Q} + \mathrm{Im}(e^{-\mathrm{i}\varphi_i}). \tag{6}$$

This form of the phase equation allows us to use the Watanabe-Strogatz ansatz [8,9], applicable to general systems of phase equations driven by a common force and having form

$$\dot{\varphi}_i = f(t) + \mathrm{Im}[G(t)e^{-\mathrm{i}\varphi_i}] \tag{7}$$

with arbitrary real $f(t)$ and complex $G(t)$ (in our case $f = I - \epsilon\dot{Q}$, $G = 1$). We use the formulation of the WS theory presented in Ref. [10]. The ensemble is characterized by three global time-dependent WS variables ρ, Φ, Ψ, and N constants of motion ψ_i (of which only $N-3$ are independent), which are related to the phases φ_i as

$$e^{\mathrm{i}\varphi_i} = e^{\mathrm{i}\Phi}\frac{\rho + \exp[\mathrm{i}(\psi_i - \Psi)]}{\rho\exp[\mathrm{i}(\psi_i - \Psi)] + 1} \tag{8}$$

with additional conditions $\sum_i \cos\psi_i = \sum_i \sin\psi_i = \sum_i \cos 2\psi_i = 0$. The equations for the global WS variables read [8–10]

$$\begin{aligned}
\dot{\rho} &= \frac{1-\rho^2}{2}\mathrm{Re}(e^{-\mathrm{i}\Phi}),\\
\dot{\Psi} &= \frac{1-\rho^2}{2\rho}\mathrm{Im}(e^{-\mathrm{i}\Phi}),\\
\dot{\Phi} &= I - \epsilon\dot{Q} + \frac{1+\rho^2}{2\rho}\mathrm{Im}(e^{-\mathrm{i}\Phi}).
\end{aligned} \tag{9}$$

To close the system we need to add the equation for Q, where the imaginary part of the order parameter Z enters, so Z should be represented through the WS variables. In general, the expression for Z is rather complex (cf. Refs. [10,11]), but in the case of a uniform distribution of the constants ψ_i, the order parameter is just $Z = \rho e^{\mathrm{i}\Phi}$. This important case, where WS global variables ρ, Φ have a clear physical meaning as the components of the Kuramoto order parameter, will be treated below. Additionally, we notice that the variable Ψ does not enter other equations, so we obtain a closed system of equations that describes the array

$$\begin{aligned}
\dot{Z} &= \mathrm{i}(I - \epsilon\dot{Q})Z + \frac{1}{2} - \frac{Z^2}{2},\\
\ddot{Q} + \gamma\dot{Q} + \omega_0^2 Q &= I - \mathrm{Im}(Z).
\end{aligned} \tag{10}$$

B. Bistability and hysteretic transitions

Analysis of system (10) is our goal in the rest of this section. Before proceeding, some remarks are in order. First, in the derivation of (10) no approximation except for an assumption of a uniform distribution of constants ψ_i has been made. The latter is a restriction on initial conditions; we discuss its relevance below. Second, the order parameter Z does not vanish in the case of full asynchrony of junctions: for noncoupled junctions with $\epsilon = 0$ we get a steady state $Z_0 = \mathrm{i}(I - \sqrt{I^2-1})$. This nonvanishing value appears because free junctions rotate nonuniformly, and the "natural" distribution of the phases in the asynchronous state is not uniform.

We start the analysis of (10) by finding its steady states. Because at such a state $\dot{Q} = 0$, the coupling vanishes and the steady state describing the asynchronous regime with

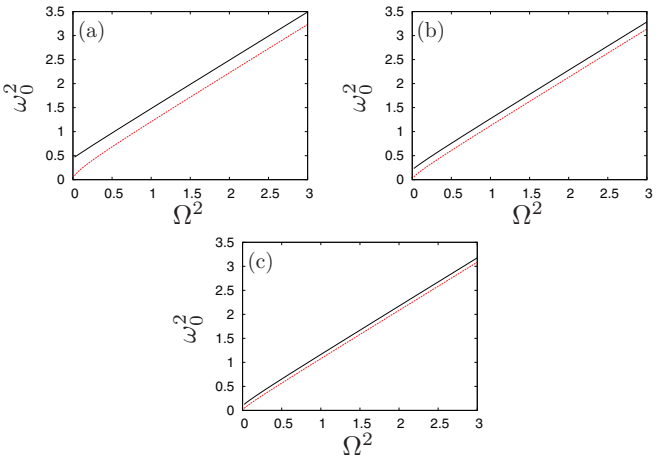

FIG. 1. (Color online) Domains of stability of synchronous (above lower dashed line) and asynchronous (below upper solid line) states on the plane of parameters (ω_0^2, Ω^2), where $\Omega = \sqrt{I^2-1}$ is the natural frequency of the junctions. Here $\epsilon = 0.5$, and $\gamma = 1.0$ (a), 1.7 (b), 2.7 (c).

$Z_0 = \mathrm{i}(I - \sqrt{I^2-1})$, $Q_0 = \omega_0^{-2}\sqrt{I^2-1}$ is the only stationary solution. Stability of this solution is determined by the fourth-order characteristic equation

$$\begin{aligned}
\lambda^4 + \gamma\lambda^3 + \left(\omega_0^2 + I^2 - 1\right)\lambda^2 + [(\gamma - \epsilon)(I^2-1)\\
+ \epsilon I\sqrt{I^2-1}\,]\lambda + \omega_0^2(I^2-1) = 0.
\end{aligned} \tag{11}$$

The stability border can be easily found by assuming $\lambda = \mathrm{i}\omega$:

$$\omega_0^2 = (I^2-1) + \frac{\epsilon}{\gamma}\sqrt{I^2-1}(I - \sqrt{I^2-1}). \tag{12}$$

The fully synchronous solution of (10) corresponds to the case $|Z| = 1$, so that only the phase Φ changes, according to the system

$$\ddot{Q} + \gamma\dot{Q} + \omega_0^2 Q = I - \sin\Phi, \quad \dot{\Phi} = I - \epsilon\dot{Q} - \sin\Phi. \tag{13}$$

We have found the limit cycle in Eq. (13) numerically and determined its stability by finding the largest multiplier. Together with expression (12) this allows us to find the domains of stability of the asynchronous and synchronous states, together with the region of bistability of these regimes; see Fig. 1.

In Fig. 2 we give another illustration of the bistability, presenting the dependence of Z_0 on parameter I, together with the value $|Z| = 1$ in the synchronous case. Here we also show what happens if our basic assumption at derivation of Eqs. (10), namely, of a uniform distribution of constants ψ_i, is not satisfied. We have simulated an ensemble of 100 junctions, preparing the initial conditions with a nonuniform distribution of constants ψ_i as described in Ref. [10], appendix C. Instead of leading to a stable state Z_0, the desynchronous population now shows an oscillating variable $Z(t)$, minima and maxima of which are marked with squares. In the synchronous regime, $|Z| = 1$ as before, and the information on the constants ψ_i gets lost as synchrony establishes.

In conclusion of this consideration we mention that we found only the fully synchronous and the fully asynchronous states in the system (10), but no partial synchronous state like

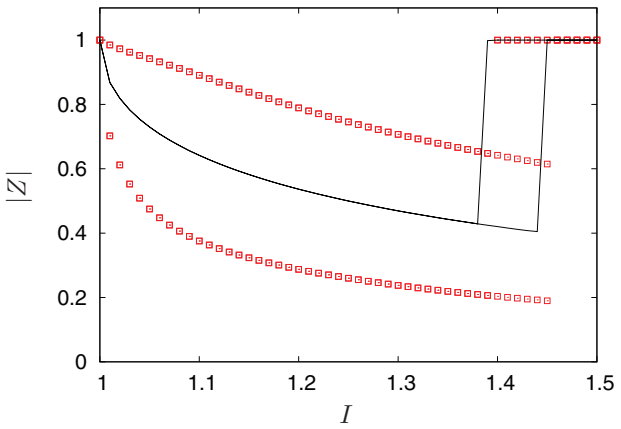

FIG. 2. (Color online) Dependence of the order parameter $|Z|$ on the current I for 100 junctions. Line: uniform distribution of constants ψ_i, squares: nonuniform distributions.

those, e.g., described in Ref. [12]. In partial synchrony the mean fields do not vanish, although the oscillators are not perfectly synchronous but form a bunch. The difference to a quite similar setup in Ref. [12] is that here we consider a linear load, while in Ref. [12] the load was nonlinear. While we cannot exclude that partial synchrony is possible for linear loads as well, our numerical study, as well as the study of Ref. [7], did not show such states.

III. NONIDENTICAL JUNCTIONS

A. Formulation of the model

There are two parameters of individual junctions that can differ: the critical current I_c and the resistance r (cf. Refs. [5,6]). In order to be able to apply the WS approach as above, we will assume that they are organized in groups, each of the size P, and the parameters of all junctions in a group are identical: the critical current is $I_c(1+\xi_k)$ and the resistance is $r(1+\eta_k)$, where index $k=1,\ldots,M$ counts the groups. The total number of junctions is $N=MP$. In this setup the equations for the junctions read

$$\dot{\varphi}_{ki} = (1+\eta_k)[I-\epsilon\dot{Q}-(1+\xi_k)\sin\varphi_{ki}],$$
$$\ddot{Q}+\gamma\dot{Q}+\omega_0^2 Q = I-\frac{1}{N}\sum_{k=1}^{M}(1+\eta_k)(1+\xi_k)\sum_{i=1}^{P}\sin\varphi_{ki}. \tag{14}$$

To each group the WS ansatz as described in the previous section can be applied, and as a result instead of the identical array equations (10) we obtain a system

$$\ddot{Q}+\gamma\dot{Q}+\omega_0^2 Q = I-\langle(1+\eta_k)(1+\xi_k)\mathrm{Im}(Z_k)\rangle,$$
$$\dot{Z}_k = (1+\eta_k)\left[\mathrm{i}(I-\epsilon\dot{Q})Z_k+(1+\xi_k)\frac{1-Z_k^2}{2}\right], \tag{15}$$

where average $\langle\rangle$ is taken over all groups. Starting from (15) one can easily take a thermodynamic limit of an infinite number of groups $M\to\infty$, in this limit $Z_k\to Z(\eta,\xi)$. Then (15) reduces to an integro-differential equation that includes the distribution function $W(\eta,\xi)$ of disorder parameters ξ,η (cf. Ref. [10]):

$$\ddot{Q}+\gamma\dot{Q}+\omega_0^2 Q = I-\iint d\eta\, d\xi\; W(\eta,\xi)(1+\eta)(1+\xi)\mathrm{Im}[Z(\eta,\xi)],$$
$$\dot{Z}(\eta,\xi) = (1+\eta)\left[\mathrm{i}(I-\epsilon\dot{Q})Z+(1+\xi)\frac{1-Z^2}{2}\right]. \tag{16}$$

B. Asynchronous state and its stability

The asynchronous state is the steady state of the system (16):

$$Z_0(\eta,\xi) = \mathrm{i}\frac{I-\sqrt{I^2-(1+\xi)^2}}{1+\xi},$$
$$Q_0 = \omega_0^{-2}\iint d\eta\, d\xi\; W(\eta,\xi)(1+\eta)\sqrt{I^2-(1+\xi)^2}, \tag{17}$$

where we assume $\langle\xi\rangle=\langle\eta\rangle=0$. Remarkably, the disorder in the junction resistances (parameter η) does not influence the value Z_0, only the disorder in critical currents (parameter ξ). However, the stability of this asynchronous state depends on distributions of η and ξ. We consider two cases, with a disorder in one parameter only.

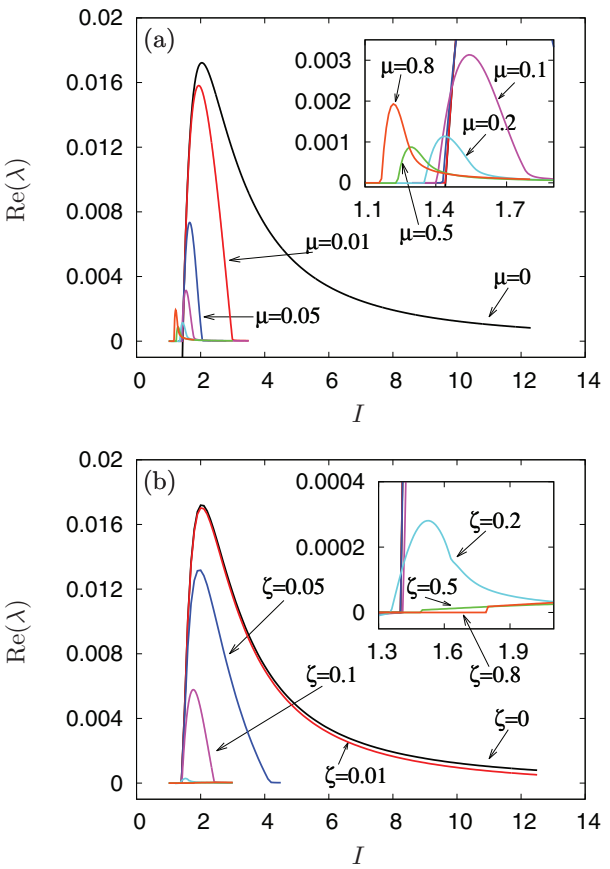

FIG. 3. (Color online) Real part of the maximum eigenvalue λ as a function of the dimensionless current I for the different values (shown on the panels) of μ (a) and ζ (b).

(1) Disorder in resistances. Here we assume that $W(\eta,\xi) = \delta(\xi)W_\mu(\eta)$ where W_μ is a uniform distribution in the interval $(-\mu,\mu)$. To study the perturbations in the integral equation (16) at the steady solution (17), we discretized the integral using 500 nodes and found the eigenvalues of the resulting matrix. The results for the maximal eigenvalue are shown in Fig. 3(a). One can see that, with increasing the external current I, the asynchronous state loses stability almost at the same critical value as for identical junctions (expression (12)), but for large values of I the stability is restored. The region of instability decreases for larger disorder μ.

(2) Disorder in critical currents. Here we assume that $W(\eta,\xi) = \delta(\eta)W_\zeta(\xi)$, where ζ is the width of the uniform distribution. With the same procedure as in case (i) we found the stability eigenvalues that are shown in Fig. 3(b). Qualitatively, the pictures look similar: both disorders result in a finite (in terms of the external current I) region of instability of the asynchronous state.

Both calculations presented in Fig. 3 show, that the main effect of disorder in arrays is in the establishing of stability of the asynchronous state for large values of current I, while only in some range (which decreases with disorder) the asynchrony is unstable. We illustrate the appearing synchrony patterns in disordered arrays in the next subsection.

C. Numerical simulations

Dynamics of the nonhomogeneous arrays of Josephson junctions is illustrated in Fig. 4. As above, we consider not a general situation where both the critical current and the resistance are spread, but cases where one of these parameters has a distribution. In numerical simulations we use the discrete representation (15). In order to avoid spurious nonsmooth solutions, an additional very small viscous term $\sim (Z_{k+1} + Z_{k-1} - 2Z_k)$ was added to the equation for Z_k that ensures numerical stabilization of the integro-differential equation.

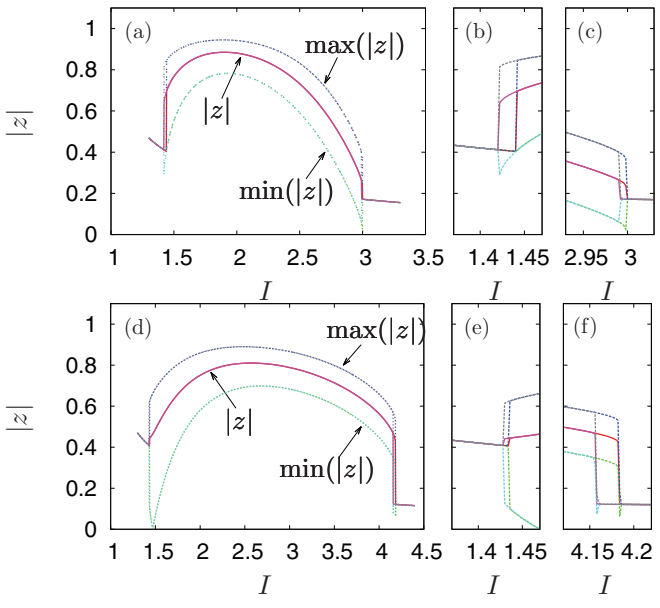

FIG. 4. (Color online) Panels (a) and (d) Dependence of the averaged order parameter $|z|$ on current I, $\mu = 0.01, \zeta = 0$, and $\mu = 0, \zeta = 0.05$, respectively. Three lines show the maximal (upper dashed line), the average (solid line), and the minimal (lower dashed line) value of variations of $|z|$ in time, in the asynchronous states these lines coincide. Panels (c), (d), (e), and (f) show enlargements of the regions near the synchrony-asynchrony transitions, to demonstrate the hysteresis.

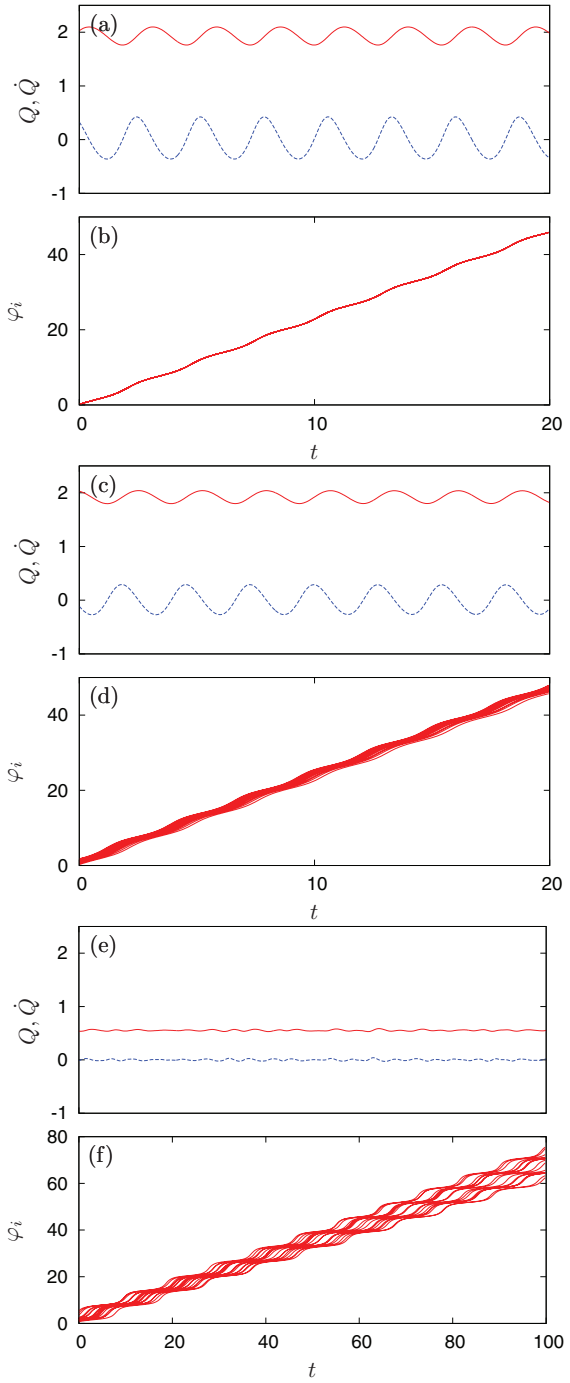

FIG. 5. (Color online) Results of simulations of an ensemble of 200 junctions for $\omega_0^2 = 1.2$, $\epsilon = 0.5$, $\zeta = 0$. In panels (b,d,f) we show only 20 phases out of 200, for better clarity. Panels (a,b): full synchrony for $\mu = 0$, $I = 2.5$. Panels (c,d): synchronous state in disordered array for $\mu = 0.01$, $I = 2.5$. Panels (e,f): asynchronous state for array with large disorder $\mu = 0.1$, $I = 1.2$.

To characterize synchrony we calculated the average over the array order parameter $z = M^{-1}\sum_k Z_k$ and plot it versus parameter I in Fig. 4. In the asynchronous state this parameter attains the fixed point [cf. Eq. (17)], while in the synchronous state it oscillates arround some mean value (because of disorder the synchrony is not complete, so $|z| < 1$). Remarkably, also in the case of disorder, the transition to synchrony demonstrates hysteresis for both small and large values of I, as can be seen in panels (b), (c), (e), and (f) of Fig. 4.

To get a flavor of how the synchronous and desynchronous states appear on the macroscopic and the microscopic level, we illustrate the dynamics of the load fields $Q, \dot{Q}$ (solid and dashed curves, respectively) and of the Josephson phases φ_i in Fig. 5. Panels (a) and (b) show complete synchrony of identical junctions. Here all the phase coincide. Panels (c) and (d) show synchronous state of junctions with a distribution of their resistances η_k. Here the phases are not identical, but form a bunch. All of them have the same frequency. In panels (e) and (f) we show an asynchronous state for larger mismatch of the resistances. Here the load fields do not oscillate what means effective absence of the coupling, and the phases of the junctions diverge, because they have different frequencies.

IV. CONCLUSION

In this paper we applied the approach by Watanabe and Strogatz to the description of the synchronization transition in an array of Josephson junctions with an LCR load. For identical junctions a closed low-dimensional system of equations for global variables (the WS variables for the junctions and two variables describing the load) demonstrates a region of bistability at the transition from asynchrony to full synchrony, so that this transition shows hysteresis. This confirms previous results based on the approximate self-consistent reduction to the Kuramoto model [7]. For nonidentical junction the method yields an integro-differential system, as each group of junctions having certain parameters is described by the WS variables. Here, with the growth of the variability of parameters, the region of synchronization shrinks. Transition to synchrony in this case is also hysteretic.

Validity of the WS approach to the Josephson junction array is based on the fact, that for standard junctions the dependence of the superconducting current on the phase is a simple sine function. Therefore, the theory is also valid for so-called π junctions [13], where the current has an opposite direction but nevertheless is propotional to $\sin(\varphi)$. However, for recently constructed so-called φ junctions [14], where the phase dependence of the current contains the second harmonics, the WS approach is not applicable, and synchronization of such junctions remains a challenging problem.

ACKNOWLEDGMENTS

V.V. thanks the IRTG 1740/TRP 2011/50151-0, funded by the DFG /FAPESP.

[1] G. Heinrich, M. Ludwig, J. Qian, B. Kubala, and F. Marquardt, Phys. Rev. Lett. **107**, 043603 (2011); M. Zhang, G. S. Wiederhecker, S. Manipatruni, A. Barnard, P. McEuen, and M. Lipson, *ibid.* **109**, 233906 (2012); A. A. Temirbayev, Z. Z. Zhanabaev, S. B. Tarasov, V. I. Ponomarenko, and M. Rosenblum, Phys. Rev. E **85**, 015204 (2012); E. A. Martens, S. Thutupalli, A. Fourrière, and O. Hallatschek, arXiv:1301.7608 (2012); M. R. Tinsley, S. Nkomo, and K. Showalter, Nature Phys. **8**, 662 (2012).

[2] A. K. Jain, K. K. Likharev, J. E. Lukens, and J. E. Sauvageau, Phys. Reports **109**, 309 (1984); S. Benz and C. Burroughs, Appl. Phys. Lett. **58**, 2162 (1991); C. B. Whan, A. B. Cawthorne, and C. J. Lobb, Phys. Rev. B **53**, 12340 (1996); A. B. Cawthorne, P. Barbara, S. V. Shitov, C. J. Lobb, K. Wiesenfeld, and A. Zangwill, *ibid.* **60**, 7575 (1999).

[3] P. Hadley, M. R. Beasley, and K. Wiesenfeld, Phys. Rev. B **38**, 8712 (1988); G. Filatrella, N. F. Pedersen, and K. Wiesenfeld, Phys. Rev. E **61**, 2513 (2000).

[4] K. Wiesenfeld and J. W. Swift, Phys. Rev. E **51**, 1020 (1995).

[5] K. Wiesenfeld, P. Colet, and S. H. Strogatz, Phys. Rev. Lett. **76**, 404 (1996).

[6] K. Wiesenfeld, P. Colet, and S. H. Strogatz, Phys. Rev. E **57**, 1563 (1998).

[7] T. Heath and K. Wiesenfeld, Ann. Phys. (Leipzig) **9**, 689 (2000).

[8] S. Watanabe and S. H. Strogatz, Phys. Rev. Lett. **70**, 2391 (1993).

[9] S. Watanabe and S. H. Strogatz, Physica D **74**, 197 (1994).

[10] A. Pikovsky and M. Rosenblum, Physica D **240**, 872 (2011).

[11] A. Pikovsky and M. Rosenblum, Phys. Rev. Lett. **101**, 264103 (2008).

[12] M. Rosenblum and A. Pikovsky, Phys. Rev. Lett. **98**, 064101 (2007).

[13] A. I. Buzdin, Rev. Mod. Phys. **77**, 935 (2005).

[14] H. Sickinger, A. Lipman, M. Weides, R. G. Mints, H. Kohlstedt, D. Koelle, R. Kleiner, and E. Goldobin, Phys. Rev. Lett. **109**, 107002 (2012).